

Statistical complexity and stochastic resonance in bistable coupled network systems excited by non-Gaussian noise

Meijuan He(何美娟), Lingyun Li(李凌云), Wantao Jia(贾万涛), and Jiangang Zhang(张建刚)
Citation: Chin. Phys. B, 2026, 35 (**3**): 030501. DOI: 10.1088/1674-1056/adfef7
http://cpb.iphy.ac.cn; http://iopscience.iop.org/cpb

What follows is a list of articles you may be interested in

A sound-sensitive neuron incorporating a memristive-ion channel

Xin-Lin Song(宋欣林), Ge Zhang(张鬲), and Fei-Fei Yang(杨飞飞)
Chin. Phys. B, 2025, 34 (**12**): 120502. DOI: 10.1088/1674-1056/ae0563

Study and circuit design of stochastic resonance system based on memristor chaos induction

Qi Liang(梁琦), Wen-Xin Yu(于文新), and Qiu-Mei Xiao(肖求美)
Chin. Phys. B, 2025, 34 (**4**): 040502. DOI: 10.1088/1674-1056/adb268

Effects of asymmetric coupling and boundary on the dynamic behaviors of a random nearest neighbor coupled system

Ling Xu(徐玲) and Lei Jiang(姜磊)
Chin. Phys. B, 2024, 33 (**6**): 060503. DOI: 10.1088/1674-1056/ad3b86

An underdamped and delayed tri-stable model-based stochastic resonance

Yan-Fei Jin(靳艳飞), Hao-Tian Wang(王昊天), and Ting-Ting Zhang(张婷婷)
Chin. Phys. B, 2024, 33 (**1**): 010501. DOI: 10.1088/1674-1056/ad01a6

Asymmetric stochastic resonance under non-Gaussian colored noise and time-delayed feedback

Ting-Ting Shi(石婷婷), Xue-Mei Xu(许雪梅), Ke-Hui Sun(孙克辉), Yi-Peng Ding(丁一鹏), Guo-Wei Huang(黄国伟)
Chin. Phys. B, 2020, 29 (**5**): 050501. DOI: 10.1088/1674-1056/ab7e9f

---

Statistical complexity and stochastic resonance in bistable coupled network systems excited by non-Gaussian noise

Meijuan He(何美娟)[1,3,†], Lingyun Li(李凌云)[1,3], Wantao Jia(贾万涛)[2], and Jiangang Zhang(张建刚)[1,3]

[1] *School of Mathematics and Physics, Lanzhou Jiaotong University, Lanzhou* 730070, *China*
[2] *School of Mathematics and Statistics, Northwestern Polytechnical University, Xi'an* 710129, *China*
[3] *Gansu Center for Fundamental Research in Complex Systems Analysis and Control, Lanzhou Jiaotong University, Lanzhou* 730070, *China*

(Received 26 May 2025; revised manuscript received 17 August 2025; accepted manuscript online 26 August 2025)

This study investigates stochastic resonance (SR) phenomena in bistable coupled networks driven by non-Gaussian noise. Employing signal-to-noise ratio (SNR) and statistical complexity as quantitative metrics, we characterize the SR behavior. First, the dimensionality of a coupled network system is reduced via the mean field theory. Subsequently, we derive closed-form analytical expressions of SNR by the path integral method, the slaving principle and the two-state model theory. Numerical simulations are used to validate the consistency between SR features identified through statistical complexity and those obtained via SNR calculations, thereby corroborating the reliability of our analytical framework. Both theoretical and numerical results conclusively demonstrate the occurrence of SR in the network system. Parametric analyses further elucidate the modulation of SR characteristics by three critical factors: non-Gaussian noise intensity parameters, noise correlation timescale and inter-node coupling strength. Finally, we explore the system's size resonance properties.

Keywords: non-Gaussian noise, bistable coupled network systems, statistical complexity measure, stochastic resonance

PACS: 05.10.Gg, 05.40.–a

DOI: 10.1088/1674-1056/adfef7 **CSTR:** 32038.14.CPB.adfef7

1. Introduction

In nature, the connections between things are often intertwined, forming an intricate network structure. Therefore, one-dimensional systems with a single variable can no longer meet the current research demands. In order to understand the complex network behavior between various things more thoroughly, researchers have gradually shifted their research focus to complex network systems.[1–4] In previous studies, Gaussian noise has been extensively investigated, leading to a series of significant results.[5–8] For example, Pikovsky *et al*. investigated an ensemble of coupled nonlinear oscillators driven by Gaussian white noise and found that the effect of system size resonance essentially relies on the presence of noise.[5] In addition, Holder *et al*. studied the stochastic Kuramoto model for phase oscillators coupled on a network, and the results showed that additive Gaussian noise acting on a more tightly coupled population allowed for improving synchronization of the other population.[6] With the development of research, people find that the noise sources are usually non-Gaussian distributed in biological, neural and physical systems, so non-Gaussian noise has a very important research value.[9–11] In particular, Gong *et al*. numerically researched stochastic complex networks with non-Gaussian noise and showed that it optimized the spiking activity of random complex networks.[9] In addition, the stochastic resonance (SR) phenomenon of nonlinear dynamical systems in the presence of non-Gaussian noise has also garnered the attention of researchers.

SR phenomenon was first proposed by Benzi and his coworkers in 1981, when they studied dynamical systems driven by periodic forcing and random perturbation.[12] Since then, the SR phenomenon has attracted wide attention and found extensive applications in the fields of science and technology, such as artificial intelligence,[13] energy harvesting,[14–16] fault diagnosis,[17,18] biological systems,[19] and neural networks.[20,21] At the same time, several methods have been proposed for quantifying the SR behavior, such as linear-response theory,[22,23] spectral power amplification[24,25] and signal-to-noise ratio (SNR).[26,27] For example, Krawiecki *et al*. proposed the majority vote model on scale-free networks and after studying the spectral power amplification of the model they found a maximum as a function of the internal noise intensity for a broad range of the model's parameters, which confirmed the occurrence of SR.[25] Wang and He derived analytically the expression of SNR in asymmetric bistable coupled network systems excited by Gaussian colored noise, and they further demonstrated the occurrence of SR phenomenon in the systems.[26] Moreover, in 2009, statistical complexity measures were proposed as a new approach to study the SR phenomena in nonlinear dynamical systems.[28] Recently, the dynamical properties of stochastic systems using the statistical complexity method were researched widely.[29–32] For example, He *et al*. used sta-

†Corresponding author. E-mail: hemeijuan@mail.lzjtu.cn

© 2026 Chinese Physical Society and IOP Publishing Ltd. All rights, including for text and data mining, AI training, and similar technologies, are reserved.

tistical complexity and Shannon entropy to study the dynamical complexity of bistable systems, and verified the accuracy of statistical complexity method using SNR.[29,30]

Based on the above discussions, it can be concluded that research results using statistical complexity are still relatively rare. In this paper, we study the SR phenomenon of a bistable coupled network system excited by non-Gaussian noise and periodic signals. In Section 2, the system is reduced and approximated to obtain the corresponding Langevin equation. After that, the adiabatic approximation theory is applied to obtain the SNR of the system. The theoretical knowledge of statistical complexity is introduced in Section 3. In Section 4, we introduce the calculation method of statistical complexity. The SR phenomenon is studied with the help of the statistical complexity approach and SNR expression and the size resonance of the system is analyzed. The results of this paper are summarized in Section 5.

2. Bistable coupled network system

Now, we consider an N-dimensional bistable coupled network system[33] driven by non-Gaussian noise and periodic signal, which is governed by the following stochastic differential equation:

$$\frac{\mathrm{d}x_i}{\mathrm{d}t} = x_i - x_i^3 + \frac{\theta}{N}\sum_{j=1}^{N}(x_j - x_i) + \eta_i(t) + S(t), \tag{1}$$

where the model is composed of N interacting bistable oscillators, each of x_i represents a single degree of freedom. θ denotes coupling constant for interaction between the oscillators, and N is the number of elements in the ensemble. $S(t) = A\cos(\omega t)$ denotes a periodic signal with the amplitude A and the frequency ω. The stochastic term $\eta_i(t)$ is non-Gaussian noise with intensity D and correlation time τ, satisfied statistical properties

$$\frac{\mathrm{d}\eta_i}{\mathrm{d}t} = -\frac{1}{\tau}\frac{\mathrm{d}}{\mathrm{d}\eta_i}V_q(\eta_i) + \frac{1}{\tau}\varepsilon_i(t), \tag{2}$$

where

$$V_q(\eta_i) = \frac{D}{\tau(q-1)}\ln\left[1 + \frac{\tau}{D}(q-1)\frac{\eta_i^2}{2}\right],$$

the parameter q denotes the extent to which non-Gaussian noise moves away from the Gaussian distribution. $\varepsilon_i(t)$ is Gaussian white noise, which satisfies properties $\langle\varepsilon_i(t)\rangle = 0$, and $\langle\varepsilon_i(t)\varepsilon_j(s)\rangle = 2D\delta_{ij}\delta(t-s)$. $\delta(\cdot)$ is the impulse function, and non-Gaussian noise $\eta_i(t)$ satisfies the following equation:

$$\begin{cases} \langle\eta_i(t)\rangle = 0, \\ \langle\eta_i(t)\eta_j(t)\rangle = \delta_{ij}\frac{2D}{\tau(5-3q)}, & q\in(-\infty,5/3), \\ \langle\eta_i(t)\eta_j(t)\rangle = \infty, & q\in[5/3,3). \end{cases} \tag{3}$$

Next, we simplify model (1) to a low-dimensional system. We define the mean field and the k-order fluctuation moments of x_i in the system are $X = \frac{1}{N}\sum_{i=1}^{N}x_i$, $M_k(t) = \frac{1}{N}\sum_{i=1}^{N}[x_i(t) - X(t)]^k$. Applying the mean-field theory[34] and Itô lemma[35] to Eq. (1), the simplified stochastic differential equations are as follows:

$$\dot{X} = X - M_3 - 3M_2X - 3M_1X^2 - X^3 + \eta(t) + S(t), \tag{4}$$

$$\begin{aligned}\frac{\dot{M}_k}{k} = {} & -M_{k+2} - 3M_{k+1}X + \left(1 - 3X^2 - \theta\right)M_k \\ & + (M_3 + 3M_2X)M_{k-1} \\ & + M_{k-1}\xi(t) + \frac{D}{5-3q}(k-1)\left(1 - \frac{1}{N}\right)M_{k-2},\end{aligned} \tag{5}$$

where $\eta(t) = \frac{1}{N}\sum_{i=1}^{N}\eta_i(t)$, $\xi(t) = -\frac{1}{N}\sum_{i=1}^{N}\eta_i(t) + \eta_i(t)$. $\eta(t)$ and $\xi(t)$ are non-Gaussian noises with intensity D, satisfying statistical properties $\langle\eta(t)\rangle = 0$, $\langle\xi(t)\rangle = 0$,

$$\left\langle\eta^2(t)\right\rangle = \begin{cases} \frac{2D}{N\tau(5-3q)}, & q\in(-\infty,5/3), \\ \infty, & q\in[5/3,3), \end{cases}$$

$$\left\langle\xi^2(t)\right\rangle = \begin{cases} \frac{2D}{N\tau(5-3q)}, & q\in(-\infty,5/3), \\ \infty, & q\in[5/3,3). \end{cases}$$

Due to the non-Markovian properties of the network system, the non-Gaussian noises in Eqs. (4) and (5) are approximated as equivalent Gaussian colored noises by using the path integral approach.[36] The non-Markov process can be written as

$$\frac{\mathrm{d}\eta(t)}{\mathrm{d}t} = -\frac{1}{\tau_{\mathrm{eff}}}\eta(t) + \frac{1}{\tau_{\mathrm{eff}}}\Gamma(t), \tag{6}$$

$$\frac{\mathrm{d}\xi(t)}{\mathrm{d}t} = -\frac{1}{\tau_{\mathrm{eff}}}\xi(t) + \frac{1}{\tau_{\mathrm{eff}}}\varepsilon(t), \tag{7}$$

where the variables $\Gamma(t)$ and $\varepsilon(t)$ are zero-mean Gaussian white noise terms with intensity D_{eff}, and statistical properties of noise terms are characterized by $\langle\Gamma(t)\Gamma(t')\rangle = \frac{2D_{\mathrm{eff}}}{N}\delta(t-t')$, $\langle\varepsilon(t)\varepsilon(t')\rangle = \frac{2D_{\mathrm{eff}}}{N}\delta(t-t')$. The noise correlation time is $\tau_{\mathrm{eff}} = \frac{2(2-q)}{5-3q}\tau$, and the noise intensity is $D_{\mathrm{eff}} = \left(\frac{2(2-q)}{5-3q}\right)^2 D$.

Applying the unified colored-noise approximation method[37] to treat the colored noises of Eqs. (6) and (7), the simplified systems (4) and (5) can be given as

$$\dot{X} = \frac{\tau_{\mathrm{eff}}^{-1}}{\tau_{\mathrm{eff}}^{-1} - c'(X)}c(X) + \frac{\tau_{\mathrm{eff}}^{-1}}{\tau_{\mathrm{eff}}^{-1} - c'(X)}\Gamma(t), \tag{8}$$

$$\frac{\dot{M}_k}{k} = \frac{\tau_{\mathrm{eff}}^{-1}}{\tau_{\mathrm{eff}}^{-1} - kd'(X)}d(X) + \frac{\tau_{\mathrm{eff}}^{-1}}{k\tau_{\mathrm{eff}}^{-1} - k^2d'(X)}\varepsilon(t), \tag{9}$$

here the parameters $c(X)$ and $d(X)$ can be further expressed as $c(X) = X - M_3 - 3XM_2 - 3M_1X^2 - X^3 + S(t)$, $d(X) = -M_{k+2} + \left(1 - 3X^2 - \theta\right)M_k + (M_3 + 3M_2X)M_{k-1} - 3M_{k+1}X + \frac{D}{5-3q}(k-1)\left(1 - \frac{1}{N}\right)M_{k-2}$.

The nonlinear terms in Eqs. (8) and (9) are simplified according to the equivalent nonlinearization method.[38] Let $f(X)=\frac{\tau_{\rm eff}^{-1}}{\tau_{\rm eff}^{-1}-c'(X)}$, $g(X)=\frac{\tau_{\rm eff}^{-1}}{\tau_{\rm eff}^{-1}-kd'(X)}$, and the approximate model is obtained by Taylor-expanding at $X=0$ as

$$\dot{X}=l_1c(X)+l_1\Gamma(t), \tag{10}$$

$$\frac{\dot{M}_k}{k}=d(X)+\frac{1}{k}\varepsilon(t), \tag{11}$$

with $l_1=\frac{\tau_{\rm eff}^{-1}}{\tau_{\rm eff}^{-1}-1}$.

To overcome the difficulty of a large number of coupled oscillators, define the cumulants of fluctuation as $K_n=M_n-\sum_{k=1}^{n-1}\frac{(n-1)!}{k!(n-1-k)!}K_{n-k}M_k$. At $n\geq 3$, all cumulants K_n exactly vanish, so assuming $n=2$, the stochastic differential equation for X and K_2 are

$$\dot{X} = l_1\left[X-K_3-3K_2X-3K_1X^2-X^3+S(t)\right]+l_1\Gamma(t), \tag{12}$$

$$\frac{\dot{K}_2}{2} = -K_4-3K_2^2-3K_3X+\left(1-3X^2-\theta\right)K_2 + \frac{D}{5-3q}\left(1-\frac{1}{N}\right)+\frac{1}{2}\varepsilon(t), \tag{13}$$

with $l_1=f(0)=\frac{\tau_{\rm eff}^{-1}}{\tau_{\rm eff}^{-1}-1}$. To obtain an analytical formula, Eqs. (12) and (13) are approximated and simplified using Gaussian approximation[39] and slaving principle. The Langevin equation can be described as follows:

$$\dot{X}=-U'(X)+l_1\Gamma(t)+l_1S(t), \tag{14}$$

where the double-well potential $U(X)=-\frac{a}{2}l_1X^2+\frac{b}{4}l_1X^4$ has two stable states $X_1=\sqrt{a/b}$, $X_2=-\sqrt{a/b}$ and an unstable state $X_3=0$, with

$$a=1+\frac{1}{2}(\theta-1)-\frac{1}{2}\left[(\theta-1)^2+\frac{12D}{5-3q}\right]^{\frac{1}{2}},$$

$$b=-\frac{1}{2}+\frac{3}{2}(\theta-1)\left[(\theta-1)^2+\frac{12D}{5-3q}\right]^{-\frac{1}{2}}.$$

The Fokker–Planck equation can be derived from Langevin equation (14), which has the following form:

$$\frac{\partial\rho(X,t)}{\partial t} = -\frac{\partial}{\partial x}\left(\tilde{A}(X)\rho(X,t)\right) + \frac{1}{2}\frac{\partial^2}{\partial x^2}\left(\tilde{B}(X)\rho(X,t)\right), \tag{15}$$

where

$$\tilde{A}(X)=l_1\bar{A}(X)=l_1\left[aX-bX^3+A\cos(\omega t)\right],$$

$$\tilde{B}(X)=l_1^2\bar{B}(X)=l_1^2\frac{2D_{\rm eff}}{N}.$$

Let $\frac{\partial\rho(X,t)}{\partial t}=0$, and integrate with

$$\rho(X)=\tilde{N}\exp\left[-\frac{\Phi}{l_1\cdot D_{\rm eff}/N}\right], \tag{16}$$

where the generalized potential function is

$$\Phi=l_1\frac{D_{\rm eff}}{N}\ln\tilde{B}(X)-\int\bar{A}(X)\,{\rm d}X.$$

Under the adiabatic limit,[40] the output SNR of the system can be expressed as

$$\mathrm{SNR}=\frac{A^2l_1^2a^2N^2}{\sqrt{2}bD_{\rm eff}^2}\exp\left(-a^2N/4bD_{\rm eff}\right). \tag{17}$$

3. Statistical complexity measure

Shannon entropy describes the uncertainty of a physical process through probability distribution $P=\{p_i,i=1,\ldots,n\}$ and is one of the classical information theoretic measures. It is defined by the form

$$S[P]=-\sum_{i=1}^{n}p_i\ln(p_i), \tag{18}$$

of the normalized Shannon entropy

$$H[P]=\frac{S[P]}{S_{\max}}, \tag{19}$$

where $S_{\max}=S[P_{\rm e}]=\ln n$, the uniform distribution $P_{\rm e}=\{1/n,\ldots,1/n\}$. The statistical complexity measure takes the functional form as follows:

$$C[P]=H[P]\cdot Q[P], \tag{20}$$

and $Q[P]$ is given as

$$Q[P]=Q_0\cdot J[P,P_{\rm e}], \tag{21}$$

$$J[P,P_{\rm e}]=\{S[(P+P_{\rm e})/2]-S[P]/2-S[P_{\rm e}]/2\}, \tag{22}$$

where Q_0 is a normalization constant.

4. Stochastic resonance

In this section, SNR, statistical complexity, and normalized Shannon entropy are applied to study SR phenomenon of an N-dimensional bistable coupled network system under the excitation of non-Gaussian noises. We employ the second-order Runge–Kutta algorithm to solve the response of coupled network system. The Bandt–Pompe algorithm is used to calculate the probability distribution of the consecutive residence time interval series.

4.1. Occurrence of stochastic resonance

The plots of statistical complexity measure, normalized Shannon entropy, and SNR under noise intensity D are presented in Fig. 1. It is shown in Fig. 1(a) that the curve of statistical complexity enhances to a maximum value and then gradually decreases, which indicates that the symbol of SR phenomenon is generated. According to the definition of statisti-

cal complexity, it can be seen that the degree of intricate patterns of bistable coupled network system gradually strengthens with the increase of noise intensity and reaches a maximum degree. Subsequently, it will become weaker as noise intensity D increases further. Correspondingly, in Fig. 1(b), with the increment of noise intensity D, the curve of normalized Shannon entropy decreases at first, and then increases. The non-monotonic curve of normalized Shannon entropy indicates that the motion of the coupled network system reaches some degree of order, and then this state is destroyed. Furthermore, in order to better show the results of statistical complexity and normalized Shannon entropy curve, SNR is given in Fig. 1(c). The SNR has a maximum value with the increase of noise intensity D, presenting the non-monotonic structure. This phenomenon is a typical characteristic of SR, indicating that SR phenomenon has occurred in the system. By comparing these figures, the trends of statistical complexity curve and the normalized Shannon entropy curve are approximately consistent with the SNR curve. It is also shown in Figs. 1(a) and 1(b) that each curve has a smaller peak, which indicates the presence of some subtle SRs.

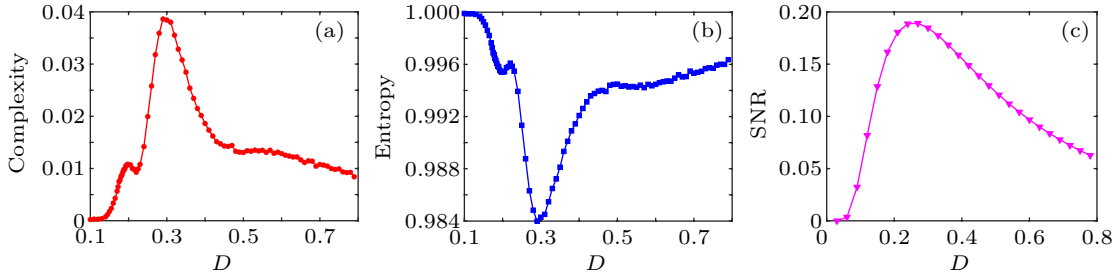


Fig. 1. (a) Statistical complexity, (b) normalized Shannon entropy and (c) SNR as a function of noise intensity D with $A = 0.15$, $\theta = 4$, $q = 0.9$, $\tau = 0.1$, $N = 2$.

4.2. Effects of parameters

In this section, the effects of non-Gaussian noise, system parameters and periodic signals on SR behavior of N-dimensional bistable coupled network models are discussed.

Further studies are carried out to explain the effect of non-Gaussian noise parameter q on SR phenomenon in Fig. 2. With the increase of noise intensity D, each statistical complexity curve has a maximum in Fig. 2(a), which illustrates the occurrence of SR. Additionally, we also observe that the peak values of statistical complexity curves increase as non-Gaussian noise parameter q increases. The peak positions shift to the left of the horizontal axis. That is, the increase of non-Gaussian parameter q can lead to the strengthening of SR behavior of coupled network system. Conversely, the peak values of normalized Shannon entropy curves decrease gradually with increasing non-Gaussian noise parameter q in Fig. 2(b). It is also seen that the peak locations of normalized Shannon entropy shift to the left side of the axis. It can also be seen that the non-Gaussian parameter q significantly influences SR phenomenon. In addition, in Fig. 2(c), as noise intensity D increases gradually from 0.02 to 0.8, each curve of SNR exhibits a non-monotonic evolutionary trend for different non-Gaussian parameters q, indicating that the system exhibits SR phenomenon. Furthermore, the peak values of SNR curves increase with increasing non-Gaussian noise parameter q, and the peak positions shift to left of the axis. By comparing the above conclusions, we can find that these simulation conclusions are consistent with theoretical SNR results.

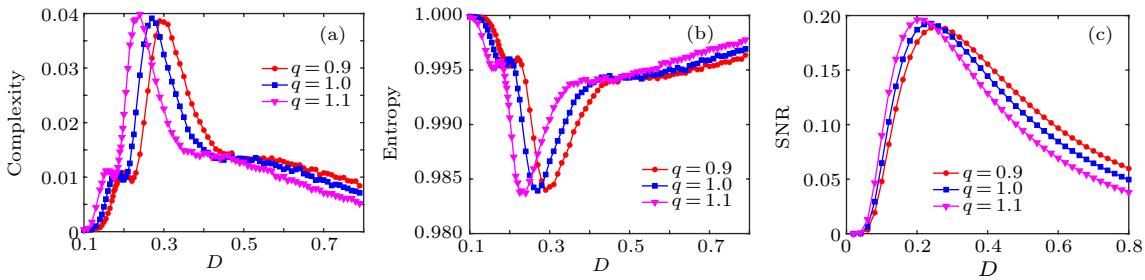


Fig. 2. (a) Statistical complexity, (b) normalized Shannon entropy, and (c) SNR as a function of noise intensity D with different values of non-Gaussian noise parameter q with $A = 0.15$, $\theta = 4$, $\tau = 0.1$, $N = 2$.

The variations of statistical complexity, normalized Shannon entropy and SNR curves with noise intensity D for different non-Gaussian noise correlation time τ are discussed in Fig. 3. The curves of statistical complexity and normalized Shannon entropy are plotted versus noise intensity D for different values of τ in Figs. 3(a) and 3(b). It is found that a single peak of each statistical complexity curve or each normalized Shannon entropy curve demonstrates the occurrence of SR. As

the value of τ increases, the maximum of statistical complexity curve rises, whereas the peak value of normalized Shannon entropy decreases. Obviously, one can see that the peak locations exhibit deviation towards the left side of the axis. That is, increasing the correlation time τ can enhance SR behavior of system. In addition, SNR as a function of noise intensity D is presented in Fig. 3(c). Each SNR curve has a peak with an optimal noise intensity D, which is considered to characterize the phenomenon of SR structure. Moreover, the maximum value of SNR curve increases as the correlation time τ increases, and the peak positions shifts slightly to the left of axis. It is easy to conclude that SR phenomenon is enhanced by increasing noise correlation time τ.

In Fig. 4, the curves of statistical complexity, normalized Shannon entropy, and SNR are demonstrated as a function of non-Gaussian noise intensity D for different coupling constant θ. On the one hand, these curves of statistical complexity and normalized Shannon entropy are non-monotonic in Figs. 4(a) and 4(b). The maximum value of the statistical complexity curve reaches the highest point and then falls while increasing θ. Obviously, the trends of normalized Shannon entropy curves are opposite. The locations of the peaks first move in the direction of increasing noise intensity and then move slightly in the direction of decreasing noise intensity. This indicates that the larger θ will suppress SR phenomenon. On the other hand, in Fig. 4(c), for any value of θ, the curves of SNR consistently exhibit a non-monotonous structure as noise intensity D increases and SR behavior is present. The SNR peak increases first and then decreases when the value of coupling constant θ increases from 2.1 to 6.9. Namely, selecting the appropriate coupling constant θ can promote SR phenomenon.

Figure 5 displays the curves of statistical complexity, normalized Shannon entropy, and SNR against noise intensity D at varying periodic signal amplitude A. Note that the curves of statistical complexity, normalized Shannon entropy, and SNR first increase rapidly and then decrease when noise intensity D increases, which reveals SR behavior. Moreover, under higher signal amplitude levels, the peaks of statistical complexity and SNR curves exhibit rapid growth, and the curves of normalized Shannon entropy present a contrasting pattern. These phenomena show that SR behavior is enhanced by larger periodic signal amplitude A.

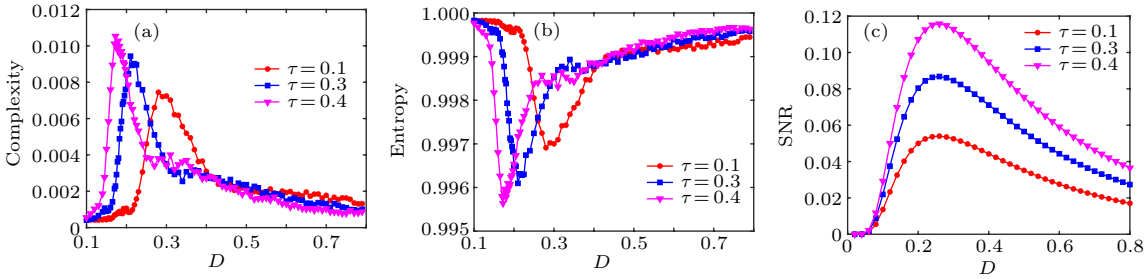


Fig. 3. (a) Statistical complexity, (b) normalized Shannon entropy, and (c) SNR as a function of noise intensity D with different values of noise correlation time τ with $A = 0.08$, $\theta = 4$, $q = 0.9$, $N = 2$.

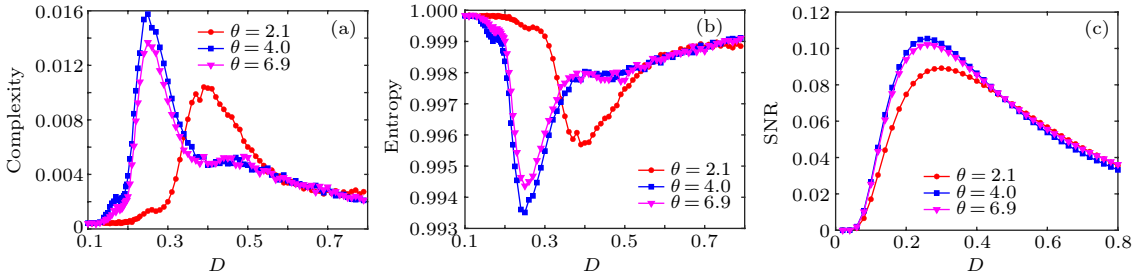


Fig. 4. (a) Statistical complexity, (b) normalized Shannon entropy, and (c) SNR as a function of noise intensity D with different values of coupling constant θ with $A = 0.1$, $q = 0.9$, $\tau = 0.2$, $N = 2$.

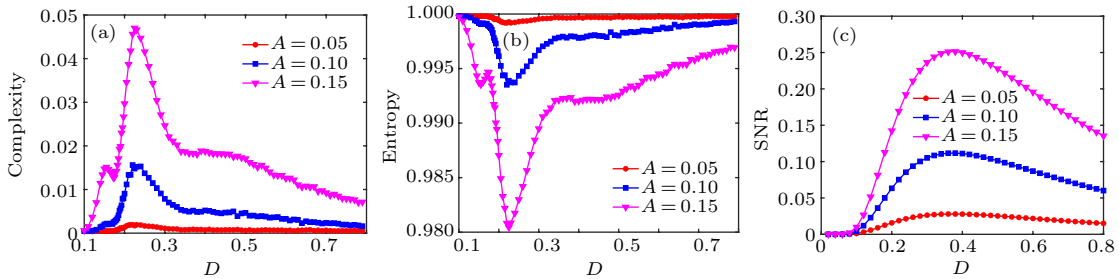


Fig. 5. (a) Statistical complexity, (b) normalized Shannon entropy, and (c) SNR as a function of noise intensity D with different values of periodic signal amplitude A with $\tau = 0.2$, $\theta = 4$, $q = 0.9$, $N = 3$.

4.3. Robustness

Next, we will discuss the influences of embedding dimension and residence time interval series length on the robustness of the numerical results. Clearly, the values of the complexity measure curves depend on the length of the residence time interval series as shown in Fig. 6(a). The shapes of the three curves show no significant change and maintain their bimodal structure under different series lengths. Moreover, the curves of the statistical complexity measures versus noise intensity D are given with different values of embedding dimension d in Fig. 6(b). It can easily be seen that these curves show small variations in shape, but all produce SR. In conclusion, the simulation results are robust with respect to the value of length M and d. This phenomenon indicates that when the condition $M \gg d$ holds true, the length M of the residence time interval sequence does not affect the occurrence of SR phenomenon in the system, and it can also prove the robustness of the Bandt–Pompe algorithm.[40]

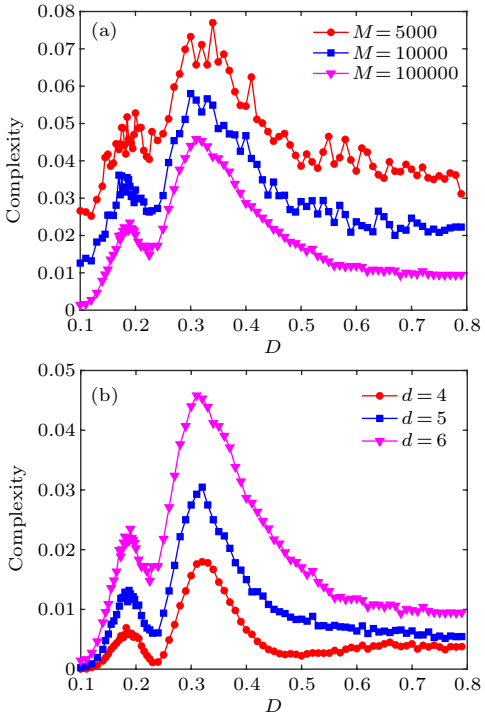


Fig. 6. Statistical complexity as a function of the noise intensity with different (a) residence time interval series length M and (b) embedding dimension d with $A = 0.2$, $\tau = 0.2$, $\theta = 4$, $q = 0.9$, $N = 2$.

4.4. System size resonance

In this section, the effects of different system parameters on size resonance are addressed by choosing parameters as $\theta = 4$. In Fig. 7, each SNR curve initially increases and then decreases with system size N, confirming the occurrence of SR phenomenon. In Figs. 7(a) and 7(d), the curve peaks rise sharply with the increase of non-Gaussian parameter q and noise intensity D, respectively, while the peak positions shift toward the direction of larger size parameter N. This indicates that increasing both non-Gaussian parameter q and noise intensity D induces the emergence of SR at larger system size N. In Figs. 7(b) and 7(c), the peak position of each curve remains invariant with modifying the parameter values, indicating that the increases of correlation time τ and signal amplitude A do not alter the system size N required for SR to occur.

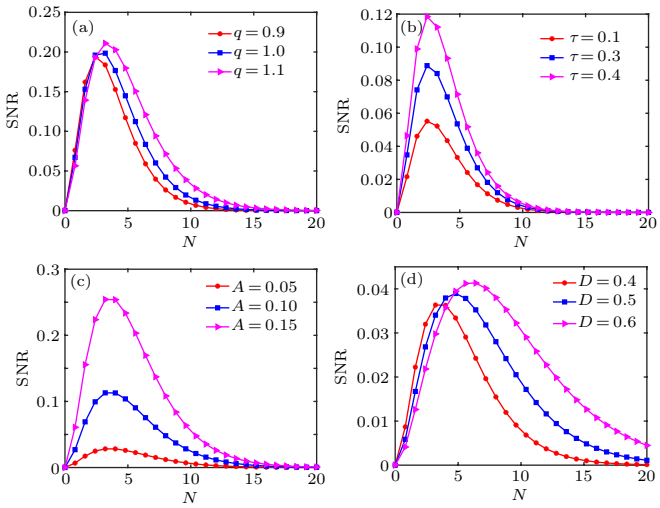


Fig. 7. SNR as a function of the system size N. (a) SNR with different values of non-Gaussian noise parameter q with $A = 0.15$, $\tau = 0.1$, $D = 0.3$. (b) SNR with different values of noise correlation time τ with $A = 0.08$, $q = 0.9$, $D = 0.3$. (c) SNR with different values of periodic signal amplitude A with $\tau = 0.2$, $q = 0.9$, $D = 0.4$. (d) SNR with different values of noise intensity D with $A = 0.05$, $\tau = 0.3$, $q = 0.9$.

The curves of SNR versus system size N for varying coupling constant θ are investigated in Fig. 8. We choose the range of coupling constant θ from 2.1 to 6.9. The shape of each SNR curve shows a non-monotonic structure, representing the appearance of SR phenomenon. In addition, the coupling constant θ increases, and the SNR peak first increases and then decreases. The position of SNR peak shifts toward the right and then toward the left. It shows that the selection of an appropriate coupling constant can promote the phenomenon of size resonance.

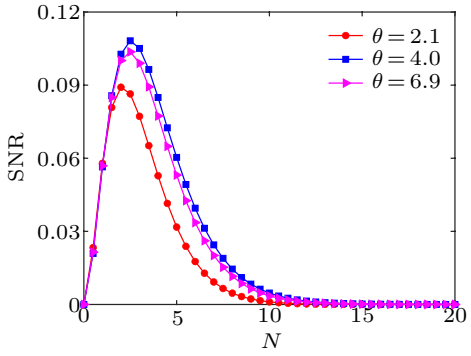


Fig. 8. SNR as a function of noise intensity D with different values of coupling constant θ with $\tau = 0.2$, $A = 0.1$, $q = 0.9$, $D = 0.3$.

5. Conclusions

To summarize, we investigate the SR problem of coupled network systems under the excitation of non-Gaussian noise. Since the systems are N-dimensional, the mean field theory is first used to decrease its dimensionality. Due to the non-

Markov nature of non-Gaussian noise, the path integral approach is used for the approximation. Thereafter, the Langevin equation corresponding to the system is obtained by applying the principle of unified colored noise approximation theory, equivalent nonlinearization method, and Gaussian approximation. Finally, SNR is derived by employing the Fokker–Planck equation under two-state model theory. By analyzing the impacts of non-Gaussian parameters, system parameters, and periodic signal on SNR and verifying numerically statistical complexity method, we draw the following conclusions. Moreover, we observe that the non-monotonic structures of SNR and statistical complexity reveal the occurrence of SR behavior. Notably, the larger non-Gaussian parameter and noise correlation time can promote SR behavior, the system is more likely to experience SR when the appropriate coupling constant is closer to 4, and increasing periodic signal amplitude will enhance the SR phenomenon of the system. In addition, the robustness of the simulated results is shown by changing the embedding dimension and residence time interval series length in the Bandt–Pompe algorithm.

In addition, the size resonance of the system is analyzed, and it is found that the increases of non-Gaussian parameter and noise intensity cause the generation of SR for larger system sizes. The larger values of noise correlation time and periodic signal amplitude will not change the system size where SR phenomenon occurs, and selecting an appropriate coupling constant can promote the size resonance phenomenon.

Appendix A

The BP algorithm was selected as the preferred method for obtaining the probability distribution because it better incorporates the time causality of the underlying system. The detailed description of the BP method is as follows:

Given a one-dimensional time series $\{x_S : s = 1, \ldots, M\}$ with embedding dimension $d > 1$, the "ordinal pattern" of order d generated by

$$(S) \to \left(x_{S-(d-1)}, x_{S-(d-2)}, \ldots, x_{S-1}, x_S\right) \tag{A1}$$

is considered. To each time s, a d-dimensional vector from the given time series at times $s-(d-1), \ldots, s-1, s$ is assigned. By the "ordinal pattern" of order d depended on the time s, the permutation $\pi = (r_0, r_1, \ldots, r_{d-1})$ of $(0, 1, \ldots, d-1)$ is defined as

$$x_{S-r_{d-1}} \leq x_{S-r_{d-2}} \leq \cdots \leq x_{S-r_1} \leq x_{S-r_0}. \tag{A2}$$

In order to obtain a unique result, BP considered that $r_i < r_{i-1}$ if $x_{s-r_i} = x_{s-r_{i-1}}$. Thus, for all $d!$ possible permutations π of order d, the corresponding probability distribution of "ordinal patterns" is expressed by

$$p(\pi) = \#\{s : s \leq \Upsilon; (s) \text{ has type } \pi\}/\Upsilon, \tag{A3}$$

where $\Upsilon = M - d + 1$, and the symbol # represents "number".

Acknowledgements

He Meijuan's research was partially supported by the Key Project of the Gansu Natural Science Foundation (Grant Nos. 24JRRA226 and 23JRRA882), Lanzhou Youth Science and Technology Talent Innovation Project (Grant No. 2024-QN-179), the Foundation for Innovative Fundamental Research Group Project of Gansu Province, China (Grant No. 25JRRA805), the National Natural Science Foundation of China (Grant Nos. 11602184 and 62463016), the Industrial Support and Guidance Project of Colleges and Universities of Gansu Province (Grant No. 2024CYZC-23), and Tianyou Youth Talent Lift Program of Lanzhou Jiaotong University.

References

[1] Dorogovtsev S N, Goltsev A V and Mendes J F F 2008 *Rev. Mod. Phys.* **80** 1275
[2] Geier C, Stender M and Hoffmann N 2024 *J. Sound Vib.* **590** 118544
[3] Li L, Jiang W and Tu Z 2023 *Appl. Math. Model* **119** 54
[4] Böttcher L and Porter M A 2024 *Phys. Rev. E* **109** 024314
[5] Pikovsky A, Zaikin A and de La Casa M A 2002 *Phys. Rev. Lett.* **88** 050601
[6] Holder A B, Zuparic M L and Kalloniatis A C 2017 *Physica D* **341** 10
[7] Ji Y, Gong Y, Su S and Bai X 2021 *Complexity* **2021** 6680287
[8] Liu Q, Xu Y, Xu C and Kurths J 2018 *Appl. Math. Model* **64** 249
[9] Gong Y, Hao Y, Xie Y, Ma X and Yang C 2009 *Biophys. Chem.* **144** 88
[10] Jia W, Feng X, Hao M and Ma S 2024 *Chaos Soliton Fract.* **185** 115134
[11] Shi T T, Xu X M, Sun K H, Ding Y P and Huang G W 2020 *Chin. Phys. B* **29** 050501
[12] Benzi R, Sutera A and Vulpiani A 1981 *J. Phys. A: Math. Gen.* **14** L453
[13] Harikrishnan N B and Nagaraj N 2021 *Neural Networks* **143** 425
[14] Liu D, Wu Y, Xu Y and Li J 2019 *Mech. Syst. Signal Pr.* **130** 201
[15] Huang M L, Yang Y G and Liu Y 2024 *Chin. Phys. B* **33** 060203
[16] Hang D, Ye J and Huang D 2025 *Commun. Nonlinear Sci.* **140** 108354
[17] Lei Y, Han D, Lin J and He Z 2013 *Mech. Syst. Signal Pr* **38** 113
[18] Jiang Z, Zhang G and Gao Y 2025 *Appl. Math. Model* **137** 115657
[19] Douglass J K, Wilkens L, Pantazelou E and Moss F 1993 *Nature* **365** 337
[20] Mato G 1999 *Phys. Rev. E* **59** 3339
[21] Jiao S, Gao R, Xue Q and Shi J 2023 *Chin. Phys. B* **32** 050202
[22] Dykman M I, Haken H, Hu G, Luchinsky D G, Mannella R, McClintock P, Ning C Z, Stein N D and Stocks N G 1993 *Phys. Lett. A* **180** 332
[23] Guo X and Cao T 2022 *Chin. J. Phys.* **77** 721
[24] Gammaitoni L, Hänggi P, Jung P and Marchesoni F 1998 *Rev. Mod. Phys.* **70** 223
[25] Krawiecki A and Kosiński R A 2020 *Acta Phys. Pol. A* **138** 824
[26] Wang Y and He M 2022 *Acta. Phys. Sin.* **71** 190501 (in Chinese)
[27] Guo F, Luo X, Li S and Zhou Y 2010 *Chin. Phys. B* **19** 080502
[28] Rosso O and Masoller C 2009 *Phys. Rev. E* **79** 040106
[29] He M, Xu W, Sun Z and Jia W 2013 *Int. J. Dynam. Control.* **1** 254
[30] He M, Xu W, Sun Z and Du L 2015 *Commun. Nonlinear Sci. Numer. Simul.* **28** 39
[31] Sun Z, Dang P and Xu W 2019 *Chaos Soliton Fract.* **125** 34
[32] Guo Y, Ding J and Mi L 2024 *Chaos Soliton Fract.* **179** 114380
[33] Kometani K and Shimizu H 1975 *J. Stat. Phys.* **13** 473
[34] Pikovsky A, Rateitschak K and Kurths J 1994 *Z. Physik B* **95** 541
[35] Øksendal B 2003 *Stochastic Differential Equations: An Introduction with Applications* (Berlin: Springer)
[36] Fuentes M A, Toral R and Wio H S 2001 *Phys A* **295** 114
[37] Hu G 1994 *Stochastic Forces and Nonlinear Systems* (Shanghai: Shanghai Scientific and Technological Education Publishing House)
[38] Zhu W and Cai G 2017 *Introduction to stochastic dynamics* (Beijing: Science Press)
[39] Cubero D 2008 *Phys. Rev. E* **77** 021112
[40] Grifoni M and Hänggi P 1996 *Phys. Rev. Lett.* **76** 1611